García Martínez, A.; Monsalve-Serrano, J.; Lago-Sari, R.; Fogué-Robles, Á.; Alemahdi, N.; Tunér, M.; López Pintor, D. (2021). Development of a fast-virtual CFR engine model and its use on autoignition studies. Fuel Processing Technology. 224:1-14. https://doi.org/10.1016/j.fuproc.2021.107031

Development of a fast-virtual CFR engine model and its use on autoignition studies

Antonio García [1], Javier Monsalve-Serrano[1], Rafael Lago Sari[1], Álvaro Fogué-Robles[1], Nika Alemahdi[2], Martin Tunér[2], Darío López Pintor[3]

[1]CMT - Motores Térmicos, Universitat Politècnica de València, Camino de Vera s/n, 46022 Valencia, Spain
[2]Department of Energy Sciences, Division of Combustion Engines, Lund University, P.O. Box 118, 221 00 Lund, Sweden
[3]Sandia National Laboratories, 7011 East Avenue, Livermore, California, United States of America

Fuel Processing Technology
Volume 224, 15 December 2021, 107031
https://doi.org/10.1016/j.fuproc.2021.107031

Corresponding author (*):
Dr. Antonio García (angarma8@mot.upv.es)
Phone: +34 963876559
Fax: +34 963876559

Abstract

Homogenous charge compression ignition engines have been studied as an alternative to the conventional diesel combustion to attain high efficiency with ultra-low NOx and soot emissions for a wide variety of fuels. However, its usage in real applications has been restricted due to the difficulties regarding combustion control and operating range extension. The modification of the fuel characteristics may be a pathway to solve the previous hurdles. Therefore, this research presents a relevant methodology to assess the fuel response to HCCI boundary conditions based on 0-D and 1-D modelling for detailed chemistry solution and state conditions definition, respectively. The results suggest that the methodology can predict the early stages of the fuel oxidation with good accuracy. For the objective of predicting the start of combustion, the best results are obtained using tabulated chemistry when investigating fuels that have pre reactions and a low temperature heat release. As the oxidation process progresses, the deviation of the pressure-temperature trajectory from non-reactive to reactive conditions after the low temperature heat release decreases the predictive capability to some extent. Nonetheless, the methodology outcomes are still valid as a qualitative metric for reactivity determination as well as the intermediate and high temperature ignition delay.

Keywords

Cooperative Fuel Research engine; HCCI; Engine modelling; Chemical kinetics; Auto ignition.

1. Introduction

Energy transition and the best energy vector for the automotive sector have been subjects of discussion in the last years. While the demand of electric vehicles has been continuously rising, its market share is still not comparable to those of conventional vehicles using internal combustion engines [1]. Different projections have reported that internal combustion engines will still be responsible for more than 80% of the total energy in the transport sector by 2040 [2] [3]. Nonetheless, significant improvements on the internal combustion engine (ICE) and aftertreatment systems technology must be accomplished to fulfil the upcoming regulations for both CO_2 and pollutant emissions [4][5]. This scenario encourages the development of advanced fuels [6] and combustion concepts aiming at both high thermodynamic efficiency and pollutant mitigation[7][8].

Significant development advancements have been achieved for internal combustion engines [9][10], attaining improvements on injection [11][12], combustion system [13][14], aftertreatment[15], and air management systems [16] which have enabled reductions of fuel consumption [17], soot and NOx emissions [18][19]. Nonetheless, among the different accomplishments, low temperature combustion (LTC) techniques are pointed as a breakthrough as they have realized a pathway to achieve high brake thermal efficiency while decoupling the emission formation mechanism of NOx and particulate matter [16]. Homogeneous charge compression ignition (HCCI) [20], Reactivity Controlled Compression Ignition (RCCI) [21][22], Dual-Mode Dual-Fuel combustion[23][24] and ϕ-sensitivity [25][26] are some of the most promising LTC techniques that have been developed in the last years. HCCI is a pioneer technique on the LTC field, having as advantages the use of a single fuel if compared to RCCI [27][28]. Nonetheless, the lack of control on the combustion development as well as the limited operating range of the engine map are some of the hurdles that have limited its implementation in real applications [29].

Recently, HCCI was restated as a potential concept for automotive applications with its introduction in a commercial engine platform by Mazda (Skyactive-X engine). The HCCI mode was enabled through an inclusion of a spark plug to enhance the combustion control, delivering significant benefits in terms of emissions and fuel consumption during driving cycle evaluations [30]. The use of HCCI operation for hybrid vehicles is also referred as a potential application due to the flexibility that is provided to the thermal engine when combined to the electric machines for the vehicle propulsion [31]. Moreover, HCCI combustion was demonstrated to be fuel flexible by several authors that combined HCCI with naphtha-like fuels, alcohols, DME, etc. [32][33]. The ability of using different fuels increases the attractiveness of HCCI since it can deal with the fuel composition variation that can be found at different regions. Additionally, it can also enable the use of low CO_2 footprint fuels as Ammonia, OMEx [34][35] and PODE[36], thus contributing to reduce the CO_2 emissions at both tank-to-wheel and well-to-wheel bases [37]. Despite the benefits and recent advances, the HCCI concept is still strongly affected by the variations of the boundary conditions and the fuel characteristics[38] [39]. The former dictates the pressure and temperature evolution inside the cylinder, which may result in different ignition quality even with small variations of the initial boundary conditions for non-sensitive fuels [40]. The second influences fundamental combustion metrics as the ignition delay and the load extension due to the appearance of knock or combustion stability (knock/stability limit)[41] [42].

The determination of the fuel response to HCCI conditions was extensively addressed in the literature. Truedsson et al. [43] have attempted to translate the fuel behavior to a single combustion metric called the Lund-Chevron HCCI number, which relates the fuel composition with the required compression ratio to attain a fixed combustion phasing, CA50 at 3 CAD aTDC. In addition, Tanaka et al. [44] investigated the effect of the fuel composition, temperature, and equivalence ratio on the HCCI combustion in a rapid compression machine, concluding that the fuel structure plays a determinant role on the ignition delay and burning rates. Later, Shibata et al. [42] identified the relation between LTHR, HTHR and engine performance through experimental engine tests. They also demonstrated that different fuel components as olefins and naphthenes can reduce the LTHR phase in the fuel oxidation. Despite the contributions from these experiments, their evaluation range was limited to few fuels at specific operating conditions, either by time limitation or experimental setup safety (pressure gradients, maximum pressure, compression ratio requirements and maximum exhaust temperatures).

In this sense, alternative methods to evaluate the fuel response to engine-like conditions were proposed during the years. Commercial reaction kinetic codes can deliver precise solution of kinetic mechanisms at specific state conditions. They can be extended to different domains from 0-D to 3-D at the expense of increasing the computational cost. Alternative solutions based on phenomenological description of HCCI combustion were also proposed along the years, aiming at reliable calculation of performance parameters. Nonetheless, they require an extensive quantity of experimental information for fitting and calibration, restricting their predictive capability. Additionally, fluid flow and thermal description are generally not based on conservative methods, being focused, generally, to the closed loop phase. Since the gas exchanges phase is neglected, the determination of quantities such as trapped residual mass must be imposed. This may result in discordances with the experimental verifications, requiring the tuning of additional settings to tailor the combustion metrics. The coupling of a reliable predictive solver to determine the in-cylinder conditions with a reaction kinetics solver may solve the limitations of the individual approach previously discussed. Nonetheless, these methodologies are not fully addressed in the literature. Different results have showed the benefits of coupling 0-D and 1-D simulations for combustion description [45][46][47]. Differently from these works, the present methodology extends the application of this coupled methodology to solve fundamental quantities such as the different ignition delays while saving significant time.

In this sense, the aim of this investigation is to develop, validate and applicate a numerical methodology to investigate the fuel response to HCCI conditions in terms of ignition delay characterisation. To do this, two contrasting fuels (ethanol and PRF63) were investigated experimentally to provide a database for the model development. This was followed by an extensive analysis to characterize the most accurate species to define low temperature, intermediate and high temperature ignition delay. These species were then used as tracking species for the Livengood and Wu method considering both full mechanism solution and ignition delay correlations, evaluating the benefits and limitations of each approach. Next, a calibrated GT-Power model was used to generate boundary conditions to assess its capability on representing engine-like conditions and the impact of not considering the in-cylinder state variation in the early phases of the combustion process.

2. Experimental materials and methodology

2.1. Modified CFR F-1 engine

CFR engines have been developed as a solution to the need of having standard methods to evaluate the combustion characteristics of fuels. Given the broad spectra of reactivity that can be found in conventional diesel and spark ignition engines fuels, two different CFR engines were developed. The CFR F-1 was designed to provide reliable information of research octane number (RON) and motor octane number (MON) values for a given fuel under controlled boundary conditions. This engine was conceptualized aiming at reproducing the geometrical characteristics of the engines of that time as it can be evidenced in Table 1. As it can be seen, the CFR F-1 presents a bore of 82.5 mm and a stroke of 114.3 mm. These characteristics are responsible for rendering the pressure and temperature evolution on the combustion chamber as well as to dictate metrics like the constant volume time.

Table 1. CFR - F1 geometrical characteristics.

Parameter	Value
Bore [mm]	82.5
Stroke [mm]	114.3
Con. rod length [mm]	254
Compression ratio	Variable from 4:1 to 18:1
TDC clearance height	(114.3)/(CR - 1)
Head/bore area ratio	1
Piston/bore area ratio	1
Wrist pin crank offset	0
Intake Valve Closing (IVC)	146 CAD bTCD
Exhaust Valve Opening (EVO)	140 CAD aTDC
Intake Valve Opening (IVO)	350 CAD bTDC
Exhaust Valve Closing (EVC)	345 CAD bTDC

During the recent years, advanced combustion concepts have been introduced aiming at exploring the limits of conventional cycles by means of combining proper in-cylinder reactivity design and pressure-temperature evolution matching. As it was stressed in the introduction, HCCI demonstrated to be one of the most promising advanced combustion concepts. Nonetheless, original CFR engines are not suitable to operate at this combustion mode. Therefore, the CFR F-1 engine was modified to enable the use of HCCI combustion. First, an electronic port fuel injector (PFI) was installed, allowing the precise control of fuel injection as well as its timing, which is fundamental for HCCI combustion stability. To do this, the original carburettor was removed, and the injector was installed in its housing, controlled by a dedicated electronic control unit (ECU). Additionally, the spark plug was disabled to avoid any energy discharge from the spark that could influence the ignition process.

2.2. Experimental facility

The CFR F-1 engine was installed in a fully instrumented test cell facility allowing to control and monitor the required boundary conditions during the tests. Figure 1 presents the schematic of the test cell facility. First, the air is conditioned by means of an air refrigerator and heater to control the humidity and the temperature, respectively. Next, the fuel is delivered by means of a PFI. The engine load is provided by means of an ABB dynamometer with maximum capacity of 30 kW and 97 Nm of torque. Finally, a Horiba Mexa 7500 is used to monitor and acquire the exhaust gas composition allowing to obtain parameters as the equivalence ratio for a given operating condition.

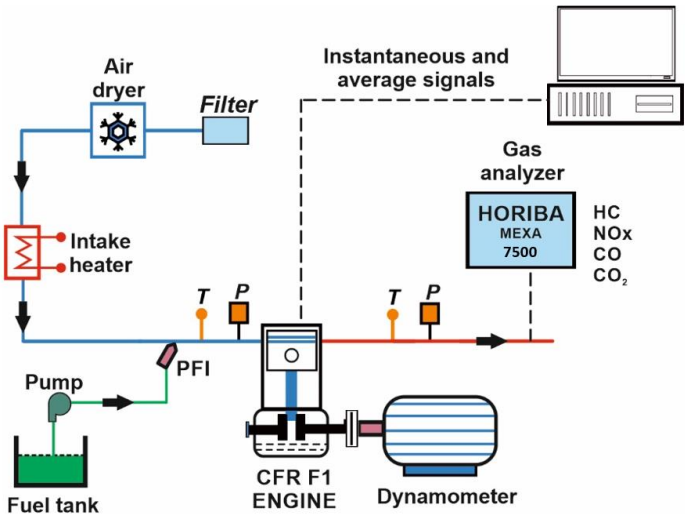

Figure 1. Experimental setup using during the CFR investigations.

In addition to this, the engine was equipped with different sensors to monitor and acquire the most relevant state conditions during the test. The instantaneous in-cylinder pressure was acquired by means of a Kistler 6125 C pressure transducer while time-averaged pressures were monitored at both intake and exhaust manifold with piezo resistive Kistler 4045A sensors. Time averaged temperature was obtained with a Pt100 thermocouple. Table 2 summarizes the uncertainty associated to each one of the measurement systems used in this investigation.

Table 2. Instrumentation with the respective measurement and principle and accuracy used to acquire the different variables of interest.

Variable measured	Device	Manufacturer / model	Accuracy
In-cylinder pressure	Piezoelectric transducer	Kistler / 6125C	±1.25 %
Intake/exhaust pressure	Piezoresistive transducers	Kistler / 4045A	±25 mbar
Temperature in settling chambers and manifolds	Thermocouple	TC direct / type K	±2.5 °C
Crank angle, engine speed	Encoder	AVL / 364	±0.02 CAD
NOx, CO, HC, O_2, CO_2	Gas analyzer	HORIBA / MEXA 7500	4%

2.3. Test methodology

The experimental campaign was designed to obtain a representative dataset for the model development and validation. To do this, an equivalence ratio sweep was performed targeting both stable operation condition as well as limiting conditions in

terms of pressure gradient and misfire. All the tests were performed at an engine speed of 900 rpm to have comparable results. Table 3 presents the different operating conditions that were assessed.

Table 3. Operating conditions and fuel properties for both Ethanol and PRF63 evaluations.

	Ethanol	**PRF63**
ρ [kg/m^3] (15ºC)	789.5	687.8
μ [mm^2/s] (40ºC)	1.056	0.56
RON/MON[-]	108.6/90.7	63/63
Formulation	C_2H_5OH	63% C8H18 + 37% n-C7H16 (%vol)
LHV [MJ/kg]	26.7	44.75
λ [-]	2.70:0.15:3.60	2.70:0.15:3.15
T_{intake} [ºC]	100, 150	50, 100, 150
P_{intake} [bar]	0.98±0.03	0.98±0.03

In an engine with a constant CR any λ variations at a constant intake temperature will shorten or longer the ignition delay respectively [25][48]. Variable CR of a CFR engine enables the adjustment and maintaining of a constant combustion phasing (e.g. CA50) while varying the ϕ. In this investigation, the compression ratio in response to the equivalence ratio and fuel variation was modified to obtain the same center of combustion for all of the operating conditions (CA50=3 CAD aTDC). In this sense, the differences in the reactivity of the different operating conditions are compensated mainly by the compression ratio instead of by the combustion development process itself.

3. Numerical tools and ignition delay background

3.1. GT-Power model definition

The determination of proper state variables during the compression stroke are of utmost importance to obtain a reliable calculation of the development of the first initiation reactions. To do this, a GT-Power model was developed for the CFR-F1 engine. In this investigation, two different simulation approaches were used.

First, a three-pressure analysis (TPA) methodology was used for calibrating the phenomenological models of heat transfer and pressure losses at different model sites. The TPA routine relies on using the instantaneous pressure traces from both intake and exhaust manifold and the in-cylinder pressure to provide information about the gas-exchange process and the closed cycle. The use of instantaneous pressure traces for the intake and exhaust conditions can be avoided by means of the complete modelling of the intake and exhaust system up to the respective environments. In spite of having drawbacks as higher simulation time, this approach is acceptable since it relies on a conservative method (finite volumes) to solve the conservation equations of mass and energy, being an alternative if the instantaneous measurement of the pressures is only available at the cylinder. The detailed description of the TPA routine can be found in previous works from the authors [49] as well as in [50]. Figure 2 depicts the model developed in GT-Power for the CFR-F1 engine, which is composed of the inlet environment, manifold and ports, the engine cylinder, and the exhaust line. The different geometries as pipe lengths and diameters were obtained from the engine

manual as well as experimental measurements. Valve discharge coefficients and lifts are those reported in [51].

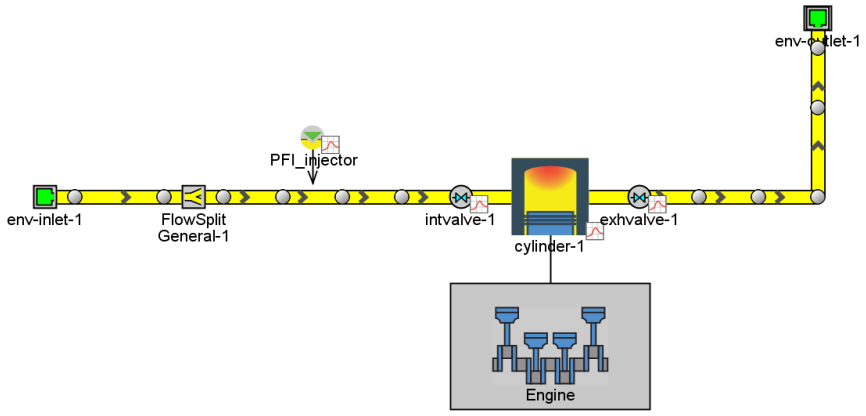

Figure 2. Numerical model developed in GT Power.

Most of the calibration process focused on the thermal characterization of the engine since the flow was demonstrated to be properly described by the model once the geometry and pressure boundary conditions are well defined. Both heat transfer and pipes require dedicate heat transfer correlations to calculate the temperature distribution and heat losses. For the pipes, the wall temperature was calculated by means of an energy balance considering the fluid properties, pipes material and environment properties for both convective and radiative heat transfer. Moreover, the pipes connected to the cylinder were set to account the heat transfer from the cylinder (thermal primitive). The cylinder thermal description was accomplished by means of a specific convective heat transfer approach proposed by Morel, Keribar and Leonard [52], which consists of a zonal heat transfer coefficient determination and a detailed wall temperature solution by means of a finite element approach.

Figure 3 depicts a pressure-volume diagram comparing the TPA results obtained with the calibrated model to those from the experiments. The figure shows a good agreement for this operating condition, even for the case of using averaged pressures at intake and exhaust, as can be evidenced on the pumping loop phase. Small differences are still visible, nonetheless, it is important to remark that the logarithm scale enhances the differences for small values. The same procedure was extended for different operating conditions, resulting in similar results.

In this sense, the calibrated model was used as a boundary condition generator for the kinetic analysis, allowing to calculate the state parameters as well as the composition of the mixture inside the cylinder during the compression stroke. This means that the models are simulated in a progressive way, where first, the whole simulation is completed in GT power and next the kinetic simulations using Cantera package (which will be described in detail in the next subsection) are performed. Despite of the advantages of this coupling methodology such as simplicity and low computational costs, some downsides must be highlighted. The model is not capable of predicting neither the state variations nor composition due to the low and intermediate temperature reactions or the high temperature heat release. In addition, the cycle-to-cycle variations that can result during the simulation from internal EGR variation are also not possible to be accounted using the proposed coupled methodology.

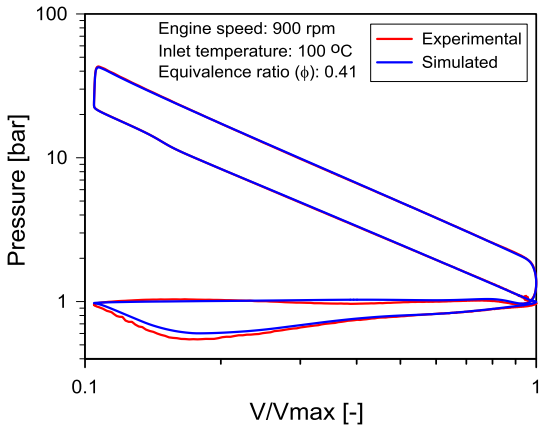

Figure 3. Pressure versus volume curve comparison for experimental and numerical results in logarithm scale.

3.2. Cantera package

Cantera was used as a reaction kinetic solver in this investigation. It is a 0-D /1-D open-source code which allows to perform different kinetic evaluations such as solving reactive systems and the determination of laminar burning velocities. Specifically, in this investigation, the solution of 0-D reactors was pursued to identify the ignition delay referred to the different temperature zones and the representative species. To do this, the closed ideal constant volume reactor was chosen allowing to solve the different state conditions that are found during the compression stroke of the CFR engine. Its formulation is based on solving the mass conservation equation for each species and the energy equation which are presented in equation 1 and equation 2, respectively.

$$m\frac{dY_k}{dt} = \sum_{in} \dot{m}_{in}\left(Y_{k,in} - Y_k\right) + \dot{m}_{k,gen} - Y_k\,\dot{m}_{wall} \qquad \text{Eq.1}$$

$$mc_v\frac{dT}{dt} = -p\frac{dV}{dt} - \dot{Q} + \sum_{in}\dot{m}_{in}\left(h_{in} - \sum_k u_k Y_{k,in}\right) - \frac{pV}{m}\sum_{out}\dot{m}_{out} - \sum_k \dot{m}_{k,gen}u_k \qquad \text{Eq.2}$$

Where, m stands for the reactor mass, V is the reactor volume, p is the reactor pressure, t is the time, T stands for temperature, Y_k is the mass fraction of each species, u is the internal energy, h is enthalpy and $\dot{Q}$ is the total heat transfer through a wall. These equations are presented in the expanded form and simplifications are done in the convenient way during the problem setup.

3.3. Reaction mechanisms

Mechanisms for fuel oxidation have been derived along the years from different experimental devices as shock tubes and rapid compression machines. The validation

range of a mechanism dictates its ability in reproducing the oxidation behavior of a fuel in that environment. As previously discussed, this research comprehends the investigation of two fuels: ethanol and PRF63 at HCCI engine conditions. This infers a wide range of pressures and temperatures as well as lean equivalence rations. Therefore, a proper mechanism must be valid for these conditions. For ethanol, previous investigations have demonstrated that the mechanism from NUI Galway is one of the best performing mechanism for engine-like conditions, having good accuracy combined with low computational cost [49]. This mechanism is composed of 113 species and 710 reactions. Despite addressing a wide number of species, it does not include specific paths for the NO_2 chemistry. This specie demonstrated to have a significant impact on the low temperature reactions. In this sense, the sub mechanism for the NO_2 reaction was included to the original mechanism. The NUI Galway mechanism has been validated in a wide range of conditions, addressing pressures from 10 bar to 50 bar, temperatures from 825 K to 985 K and equivalence ratios from 0.3 to 1 through shock tube and rapid compression machine experiments.

For the primary reference fuels (PRF) oxidation, several mechanisms are available in the literature being generally validated at engine conditions given their applicability in engine combustion development. For this research, different mechanisms were assessed aiming at identifying their capability on reproducing the experimental ignition delay. The first mechanism is the one proposed by Andrae et al. [53] which consists of 137 species and 138 reactions. This mechanism was extensively used in different investigations. Mingyuan et al. [54] presented a comprehensive comparison among several mechanism indicating that the mechanism from Andrae et al. [53] provides the best results compared to some of the recent mechanisms available for the toluene primary reference fuels (TPRF) oxidation. The second mechanism comprehends a recent mechanism developed by Sandia National Laboratories (SNL) composed of 248 species and 1428 reactions.

Figure 4 presents a brief comparison of the results from both mechanisms (Andrae and SNL) for a temperature sweep at three different equivalence ratios and pressures for a constant volume reactor. As it can be seen, significant variations on the ignition delay time are perceived. The SNL mechanism provides a much faster ignition delay at lower temperatures compared to the mechanism proposed by Andrae et al. [53]. This can be attributed to the revision and inclusion of the reaction rates of the main low temperature reactions adjusted with recent experiments carried out at Sandia National Laboratory facilities. At temperatures above the NTC, the Andrae mechanism tends to deliver shorter ignition delay times, mainly for rich conditions, while the differences between mechanisms at lean conditions for high temperature conditions are not as sensitive as those from low temperature and NTC regime.

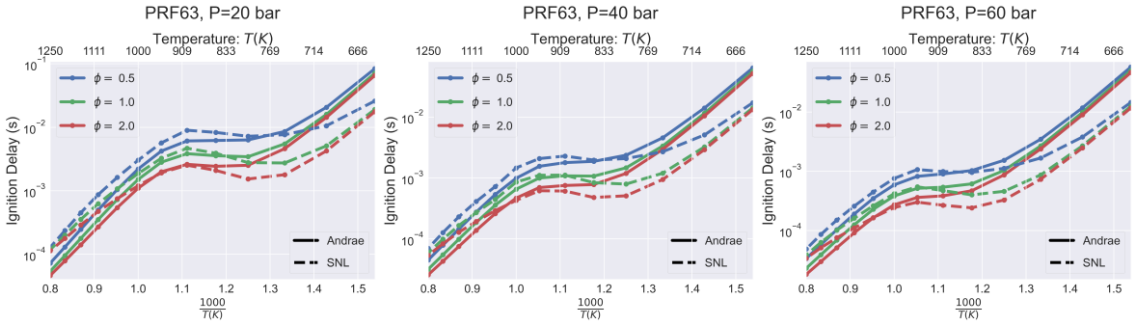

Figure 4. Differences in ignition delay prediction between both mechanisms for PRF 63 fuel.

The extension of the mechanism effect on the engine ignition delay determination is not direct since different zones may be reached during the compression and early combustion development phases. Therefore, the application of both mechanisms together with the Livengood and Wu approach is proposed to identify the accuracy of each one considering engine measurements [55].

3.4. Engine ignition delay determination

The ignition delay determination has received attention given its role on understanding the fuel chemistry and its extension to combustion control and optimization. Specifically, for internal combustion engines, the introduction of the so-called low temperature combustion concepts has emphasized the usefulness of tailoring the ignition delay to control pressure gradients and aim to extend the LTC operating ranges [56][57]. Historically, ignition delay in engine combustions was referred to as the time to obtain 2% of mass fraction burned or any predefined mass fraction burned quantity [58]. Nonetheless, this macro concept is not suitable to highlight the importance of early reactions that are fundamental to the combustion development for kinetically controlled combustion concepts. These reactions are responsible for the low temperature and intermediate temperature heat releases[59]. In this sense, a more comprehensive definition was used, following the discussion presented by Peters et al. [60]. This definition relies on defining the different temperature heat releases that can exist in a combustion development process: low temperature heat release (LTHR), intermediate temperature heat release (ITHR) and high temperature heat release (HTHR). For each one of them, an ignition delay time is associated. Figure 5 represents an illustrative heat release profile depicting the different combustion stages as well as the heat release regimes. Different methods to specify each one of the ignition delays are found in the literature. The one proposed by Waqas et al. [61] was used here, relying on a fixed threshold for the heat release profile to define the start of the different heat release zones.

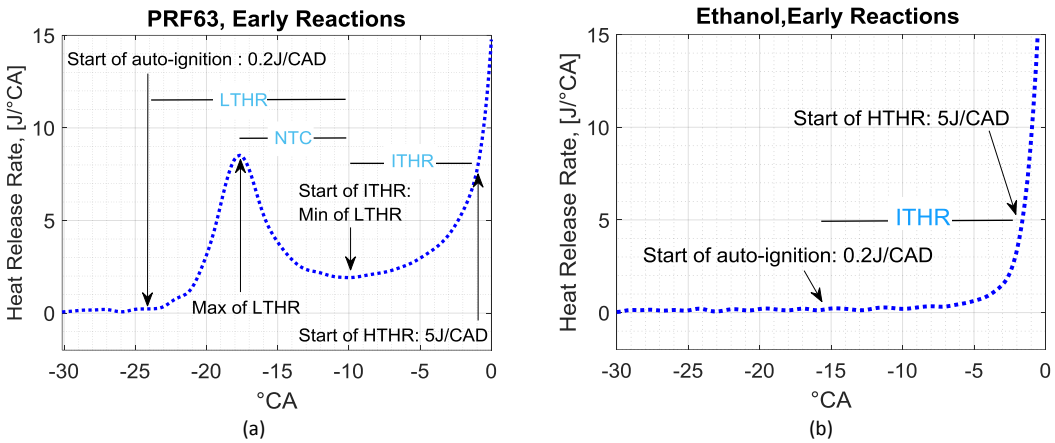

Figure 5. Criteria for differentiating low, intermediate, and high temperature heat release processes.

Finally, a method to correlate the ignition delay from each one of the simulated reactors with that from the engine should be defined. The Livengood and Wu (LW) [55] method has been extensively used to correlate the ignition delay from a specific state conditions with those from engine experiments. The LW integral consists of describing the evolution of a specific mixture towards ignition accounting the information related to the kinetics of oxidation reactions under specific pressure temperature conditions for a given mixture composition. The LW integral assumes that the amplitude of the considered ignition carriers would only increase towards its critical value at ignition according to a certain time delay τ [32]. In HCCI operation mode, the in-cylinder pressure and temperature of the air-fuel mixture that is compressed during the compression stroke should be considered to assess the concentration of the ignition carriers. Different authors have proposed reformulation of the original LW equations (Eq. 3) to account for low temperature heat release reactions and intermediate reactions. The formulations proposed by Desantes et al. [62] have demonstrated to be capable of providing a classification of the ignition delay: low, intermediate, and high temperature ignition delay. This was accomplished by employing the first equation proposed by Desantes et al. (Eq. 4) in which combustion stages are characterized by tracing an event through relevant species (ignition carriers) The determination of the species is not straightforward, and a detailed assessment of the most suitable ones to represent the low, intermediate, and high temperature ignition delay are presented in the following subsections.

$$1 = \int_0^{\tau_{ign}} \frac{1}{\tau} dt \qquad \text{Eq.3}$$

$$1 = \frac{1}{[CC]_{crit,t=t_{CC}}} \int_0^{t_{CC}} \frac{[CC]_{crit}}{\tau_{CC}} dt \qquad \text{Eq.4}$$

The determination of the ignition delay and critical concentrations of relevant tracing species has to be obtained for a wide range of operating conditions to include the effect of thermodynamic variables and compositions (pressure, temperature, relative stoichiometric ratio, EGR fraction and initial concentrations of reactive species). Even if the current study only contemplates the homogeneous mixture distribution

characteristic of HCCI combustion modes with no use of EGR, once the initial matrix of characteristic ignition delays and species concentrations is obtained, the methodology presented in this work can be adapted to any other combustion mode including effects like temperature or fuel stratification by contemplating the temporal or spatial evolution of mixture composition as well as local temperatures, depending on the amount of information available for each case and always considering that an adequate chemical model is necessary.

4. Results and discussion

4.1. Selection of mechanism and relevant species

4.1.1. Ignition delay tracers

The definition of the proper species for the different heat release tracking is fundamental to accomplish a reliable approach to correlate numerical and experimental results. To attain this, the main hydrocarbon oxidation paths should be understood. Blocquet et al. [63] have suggested that, at moderate temperatures (750 K - 950 K), the radical R, that is originated in the first initiation reactions, generally by a third body reaction, yields an unsaturated hydrocarbon (alkene) and a HO_2 radical[64]. The last generally react in a termination stage, forming hydrogen peroxide (H_2O_2). As the temperature values increase, the H_2O_2 leads to two OH radical, being a fast chain-branching reaction [65]. Another intermediate species as formaldehyde are also formed during a hydrocarbon oxidation in a broad range of temperatures [66], being rapidly consumed once the high temperature reaction starts. Therefore, these species are generally identified as good tracers for each one of the oxidation stages. It is worth to remark that other species can be also identified as chain propagators as presented in different works in the literature and may be used to identify the phases that precedes the high temperature oxidation [67][68].

However, as it is depicted in Figure 6, the formation of species as HO_2 are not only limited at low temperature reactions. In addition, other species as hydrogen peroxides and formaldehydes are formed during a wide range of temperatures. In this sense, both the species and the criteria related to the species profile must be defined, considering the phenomenon under analysis. For HO_2, the first peak is correlated with the low temperature chemistry and is the one that should be considered for determining the ignition delay. On the other hand, species as H_2O_2 and CH_2O must be related to their maximum value. As shown in Figure 2, the hydrogen peroxide peak appears at the end of the intermediate temperature reactions, indicating that its maximum value provides a reference for the last stages of intermediate heat release. Finally, both OH and CH_2O have their peak values close to each other, in conditions where the high temperature chemistry start to be dominant. Therefore, they should provide a way to compute the high temperature ignition delay.

It is worth to mention that the prediction of the evolution for the tracers is dependent on the kinetic mechanism used. Different reactions rates can lead to differences in the absolute concentration of the radicals as well as their production rate, which may result in erroneous values for the ignition delay times. In this sense, the next subsection evaluates the two mechanisms that were previously presented at different representative operating conditions.

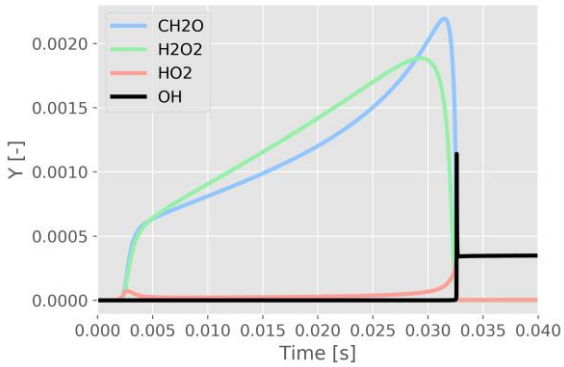

Figure 6. Species mass fraction evolution during combustion in a homogeneous reactor.

4.1.2. Mechanism effect

To investigate the mechanism impact on the determination of the ignition delay, three different operating conditions were evaluated for PRF63, addressing different intake temperatures (50°C, 100°C and 150°C) for a lambda value of 2.8. Due to the testing methodology, the compression ratio is also different for each one of the inlet temperatures. This intake temperature sweep was chosen since it can render different pressure-temperature trajectories inside the cylinder during the compression stroke. Both pressure and temperature as well as the mixture composition were obtained from the TPA calculation in GT-Power. Figure 7 presents the pressure-temperature trajectories for the three different cases. As it can be seen, the pressure-temperature trajectories are displaced from zones inside the NTC affected operation (RON-MON) space, to conditions inside the beyond MON operation as the temperature is increased, which should reduce the amount of energy released during the low temperature reactions.

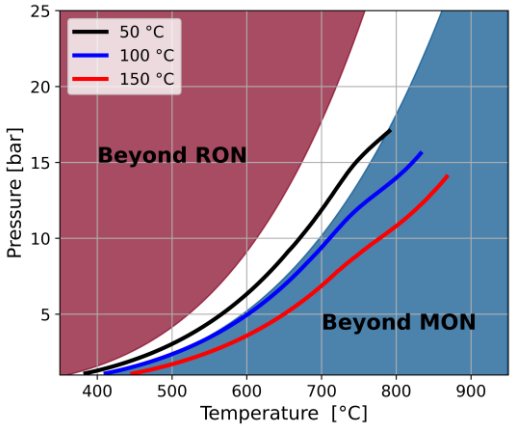

Figure 7. Pressure-Temperature trajectories at different intake temperatures.

The reduction of the LTHR can be evidenced in Figure 8, which depicts the different heat release profiles for each one of the temperatures evaluated. As it can be seen, the 50°C case has the highest LTHR peak, due to its higher residence time inside NTC affected zones. By contrast, the 150°C case has an almost flat LTHR. It is evident that the heat release profiles represent contrasting conditions in terms of engine operation and the importance of low temperature chemistry. Therefore, the pressure-temperature

trajectory and composition were used as inputs to the LW Cantera script, allowing to obtain the engine ignition delay for both mechanisms and different species. Next, they were plotted against the evolution of the heat release profiles as markers to evidence their ability in reproducing the experiments for both mechanism as presented in Figure 8.

As it can be seen, the ignition delay results are strongly dependent on the kinetic mechanism. First, the low temperature ignition delay prediction differs by more than 5 CAD between mechanisms. While the mechanism from SNL can reproduce the early phases of the ignition delay, the mechanism proposed by Andrae et al. seems to have a slow low temperature chemistry, providing a delayed ignition criterion from half to the end of the low temperature ignition delay. Other significant differences are perceived for the CH_2O, i.e., high temperature ignition delay criteria. In this case, the trend is the opposite, having earlier results for the mechanism from Andrae et al. [53] than the one verified for SNL. The predicted LW results for Andrae et al. [53] are found inside of the ITHR zone, which may infer an over prediction of the CH_2O production and early consumption. This scenario is verified for all the cases evaluated. The results allowed to conclude that the SNL mechanism can deliver a better description of the chemical reactions, given the set of boundary conditions. In this sense, the SNL mechanism was chosen to perform the remaining evaluations given its capability of predicting the characteristic times form the experimental heat release.

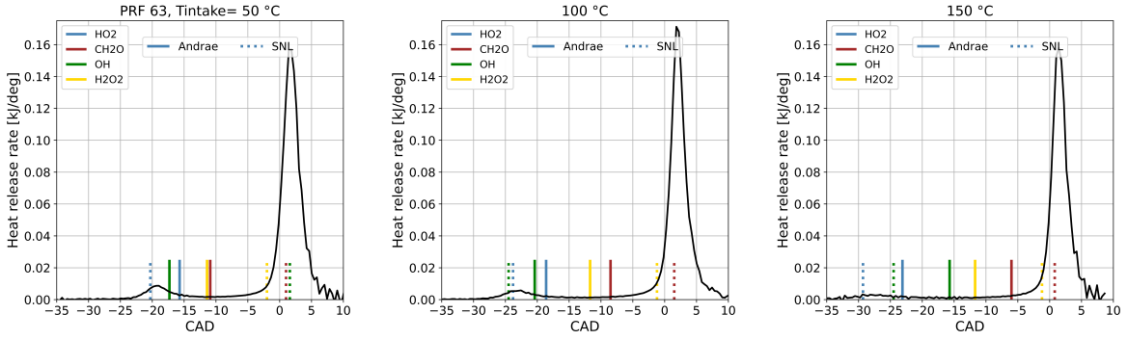

Figure 8. Ignition delay prediction capabilities of both mechanisms for PRF fuels.

4.2. Validation of LW approach

To validate the results of the LW approach, a comparison was performed against the full dataset of experiments addressing different intake temperatures and equivalence ratios. The boundary conditions that define each operating condition and their reference with the case numbers of the simulations are presented in Table 4. As it can be observed, the cases are ordered from lower to higher excess air ratio values. Ethanol cases only addresses conditions with 100°C and 150°C since lower temperatures hinders the autoignition process.

Table 4. Values of intake temperature, equivalence ratio and compression ratio for each operating condition evaluated for both Ethanol and PRF63.

Ethanol Cases														
Case Nº	0	1	2	3	4	5	6	7	8	9	10	11	12	13

T_{intake} (ºC)	100	150	100	150	100	150	100	150	100	150	100	150	100	150
λ (-)	2.70	2.70	2.85	2.85	3.00	3.00	3.15	3.15	3.30	3.30	3.45	3.45	3.60	3.0
CR (-)	14.6	12.8	14.7	12.8	14.8	12.8	14.9	12.9	14.9	13.0	15.0	13.0	15.1	13.2
PRF63 Cases														
Case Nº	0	1	2	3	4	5	6	7	8	9	10	11	-	-
T_{intake} (ºC)	100	150	50	100	150	50	100	150	50	100	150	50	-	-
λ (-)	2.70	2.70	2.70	2.85	2.85	2.85	3.00	3.00	3.00	3.15	3.15	3.15	-	-
CR (-)	9.6	9.1	10.6	9.8	9.2	10.8	10.0	9.3	11.1	10.1	9.5	11.0	-	-

For each operating condition described in Table 4 , the previously explained methodology was employed: calculation of pressure, temperature, and composition for the experiments in GT-Power coupled with the Cantera LW routine. The validation was performed for both fuels (Ethanol and PRF63), comparing the intermediate and high temperature ignition delay for the former and low, intermediate, and high temperature ignition delay for the last. Figure 9 presents the results of the comparison for ethanol for both intermediate temperature ignition delay (a) and high temperature ignition delay (b). It is worth to mention that the experimental results are always those obtained from the experimental heat release profiles considering the methodology from Peters et al. [57]. As it can be seen, a good correlation is attained for both cases. Small variations are observed, mainly for the leaner mixtures and low intake temperature. In spite of that, the differences are lesser than 1 CAD, independently on the operating condition evaluated. It is also interesting to note that both hydrogen peroxide and formaldehydes also maintains their roles on providing a reliable quantification method of each one of the oxidation stages of the ethanol concurring with that evidenced for PRF63 in the previous subsection. In addition, the proposed approach can follow, at some extent, not only the absolute values, but also the behavior evidenced in the experimental results.

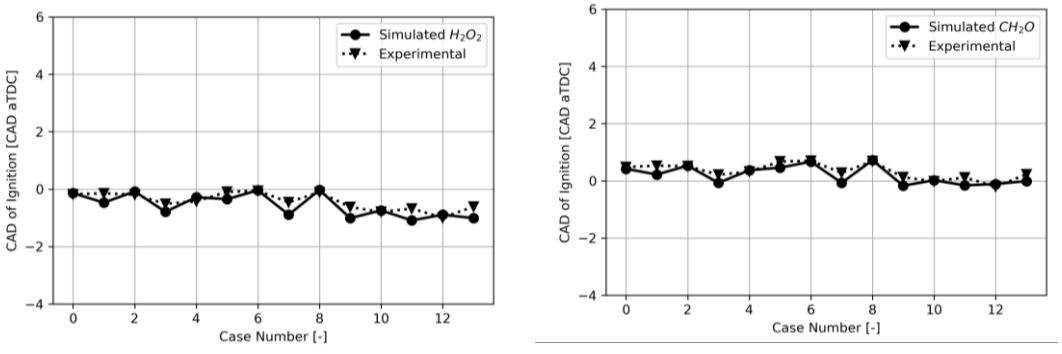

Figure 9. Comparison between experimental results and simulated predictions of the start of low temperature reactions (a) and high temperature reactions (b) for ethanol.

For PRF63, the three pre-selected species were used as representative of low, intermediate and high temperature ignition delay. First, the results of low temperature ignition delay are presented in Figure 10a. The comparison with experimental results allows to conclude that the LW approach can predict the low temperature ignition delay, considering the mechanism proposed by SNL. As it can be observed, the selection of the critical concentration of HO_2 to specify the low temperature ignition delay (LTID) provides a robust criterion, having an excellent matching, independently on the intake temperature and equivalence ratio evaluated. By contrast, the intermediate temperature zone presents higher differences between simulated and experimental

results. This zone implies a slow oxidation process with small heat release during larger periods. Therefore, small variations on the experimental criteria to define the intermediate temperature ignition delay (ITID) may result in several crank angles of difference. In addition, the small temperature and pressure gradients in this area makes it more susceptible to any discrepancies between the calculated state conditions and the real ones. These issues are decreased when the high temperature oxidation starts, since the reaction rates are enhanced, resulting in a fast temperature and pressure increase, i.e., higher gradients. This allows a proper specification of the high temperature ignition delay (HTID) and a good agreement with the maximum concentration of the formaldehyde, allowing to conclude that this species convey the kinetics background to a macro experimental parameter as the HTID.

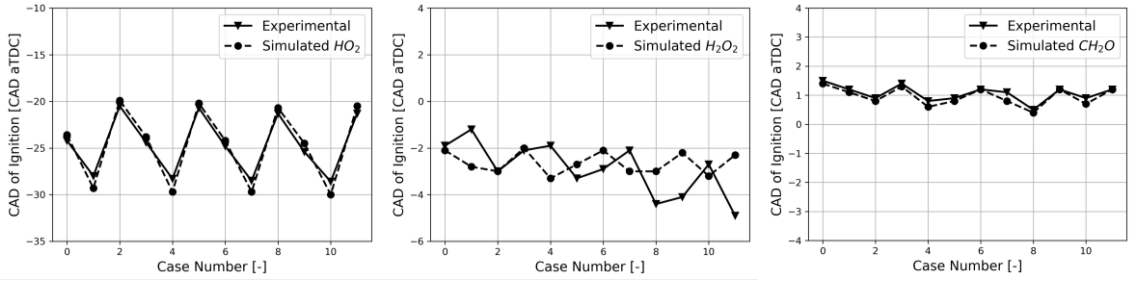

Figure 10. Comparison between experimental results and simulated predictions of the start of low temperature reactions (a), (intermediate reactions (b) and high temperature reactions (c) for PRF63.

4.3. Semiempirical correlations versus tabulated chemistry.

The LW approach time consumption is directly proportional to the time spent in obtaining the ignition delay for each one of the individual reactors and the discretization of the compression stroke. While the last cannot be decreased without losing accuracy, different solutions are proposed for the former as tabulated chemistry and semiempirical correlations, which could benefit the calculation speed of the approach. Ignition delay correlations have been extensively used, comprehending different functional dependencies, individual parameters, etc. Equation 5 presents the ignition delay correlation proposed by Shariatmadar et al. [69], which addresses some of the most fundamental properties that affects the ignition delay for a given reactor. Each one of the parameters a, b, c, d and e are used to fit the correlation considering the experimental data.

$$\tau_{ign} = a \cdot \phi^b \cdot P^c \cdot T^d \cdot e^{e/T} \qquad \text{Eq. 5}$$

The constants found in the fitting process are shown in Table 5.

Table 5. value of the different parameters for each one of the species correlations.

Parameter/species	HO_2	H_2O_2	CH_2O
A	-	$4.79 \cdot 10^{25}$	$4.31 \cdot 10^{25}$

B	-	−0.53905	−0.585421
C	-	−0.83759	−0.8406424
D	-	−10.2407	−10.160331
E	-	7524.18	7201.96763

To do this, a nonlinear fitting method was applied, providing a reasonable accuracy and fitting, which is here evaluated by means of the R-squared error (Figure 11). As it can be seen, the proposed correlation provides similar results to those from the complete mechanism solution with R^2 higher than 0.99. Small variations are perceived for small ignition delay values. It is important to remark that the logarithm scale used in the graph tends to maximize small values. Nonetheless, its performance compared to the full mechanism solution with LW should be evaluated to assess the impact of these variations on the final engine ignition delay solution.

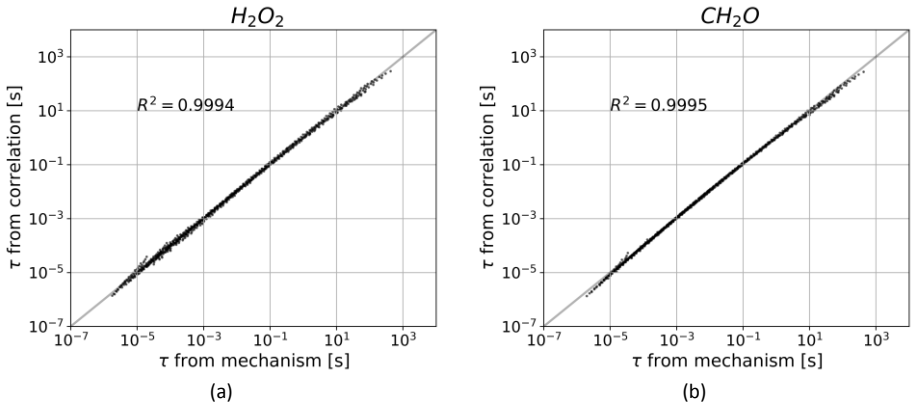

Figure 11. Fitness of adjusted correlations for different combustion stages of ethanol.

To compare the correlation performance, the LW ignition delay was recalculated considering the proposed correlation and its results were compared with those from the complete mechanism solution. As it can be observed in Figure 12, the differences are minimal, not exceeding 0.5 CAD even in the worst case. On the other hand, the time consumption in the calculation was reduced in order of magnitudes. Therefore, it can be concluded that the use of ignition delay correlations provides an alternative to speed up the calculation process of the LW integral at the cost of a small accuracy lost.

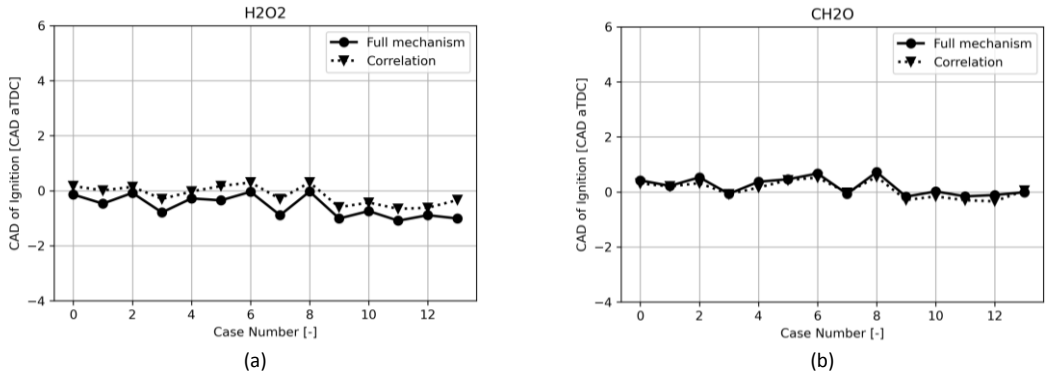

Figure 12. Evaluation of accumulated error in the prediction of different combustion stages start for ethanol when using fitted correlations.

The same nonlinear fitting method was applied was attempted to be extended to PRF63 for the different ignition delays (HO_2 for LTHR, H_2O_2 for ITHR and CH_2O for HTHR). However, in this case, the correlation fitting was not as successful as that for the ethanol. This can be evidenced in Figure 13, where the results from the mechanism solution are compared against those from the best fitted correlation, applying Equation 4 and by considering the R^2 values presented in the Figure. As depicted, there is a high dispersion, demonstrating the inability of the correlation in capturing the non-monotonicity of the ignition delay with respect to temperature, pressure and equivalence ratio caused by the LTHR that some conditions may present. Alternative formulations have been presented along the years for delivering best fitting for fuels with NTC as the one proposed by Delvescovo et al. [70]. Nonetheless, they are fundamentally based on considering a high number of adjusting factors, instead of providing a phenomenological modelling of the problem.

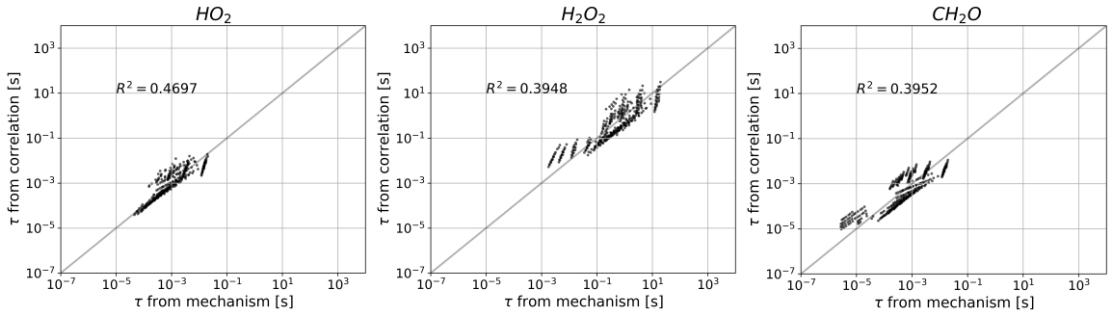

Figure 13. Fitness of adjusted correlations for different species considering the full mechanism solution and the fitted ignition delay correlation for PRF 63.

An alternative approach relies on employing tabulated chemistry considering pre-defined ranges of equivalence ratio, temperature, and pressure for each fuel. Despite a computational costly approach at first instance, since points that may not be used are still computed, this approach can pay-off for continued usage. Due to this, tabulated chemistry has been extensively used in last years to enhance the computational speed and to enable close to real time simulations. In this sense, once the tables are prepared, the ignition delay of the individual reactors can be easily determined by means of look up interpolation methods. Therefore, the ignition delays were pre-calculated for both ethanol and PRF63 and, therefore, used in the LW routine.

Figure 14 summarizes the results obtained considering the full mechanism, correlation and tabulated chemistry approaches as well as their differences compared to the experimental results for both ethanol (Figure 14a) and PRF63 (Figure 14b). It is worth to mention that the PRF63 correlation was not included in the comparison due to the poor results that are get form its application. The analysis of the results for both ethanol and PRF63 allows to conclude that the use of the tabulated chemistry provides similar results compared to those of the full mechanism solution. Small modifications are observed in leaner conditions, which may be attributed to the discretization used to create the tables ($\Delta\phi$=0.05, ΔT=20 K and ΔP= 5 bar). From the set of methodologies evaluated, it can be inferred that the use of tabulated chemistry for determining the individual ignition delay correlations provides the best results compared to the full mechanism

solution, being able to deliver reasonable accuracy for fuels with and without NTC occurrence.

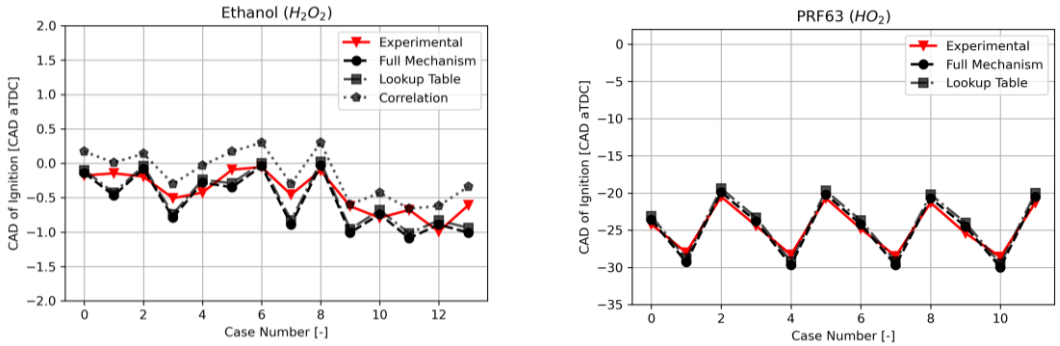

(a) (b)

Figure 14. Comparison of start of combustion prediction capability when solving all chemistry, using a lookup table or fitted correlations for ethanol (a) and PRF63 (b).

4.4. Validity of GT power model

Finally, the validation of GT Power as a boundary condition generator for LW analysis is tested at different operating conditions for both fuels. First, the pressure and temperature trajectories of both ethanol and PRF63 obtained from the non-reactive compression stroke simulation with GT power are compared with those from the experiments, to evidence the benefits and limitations of the approach. Next, the impact of using this approach is compared on an ignition delay basis for both fuels.

Figure 15 shows the pressure trajectory comparison for both ethanol (a) and PRF63 (b). As it is shown, the pressure temperature trajectory from the simulation is like that from the experiments during most of the compression stroke independently on the fuel. However, as the early reactions starts to occur, deviations can be evidenced in the trajectory. The most noticeable changes are found at the PRF63 cases, due to the significant heat released in low temperature conditions. This heat released increases the temperature, decoupling it from the non-reactive one. Consequently, the prediction of the intermediate and high temperature heat release may be affected. Nonetheless, the main goal of this study is to provide a tool to investigate the fuel response to the boundary conditions considering the early reactions and, therefore, the differences should be minimal.

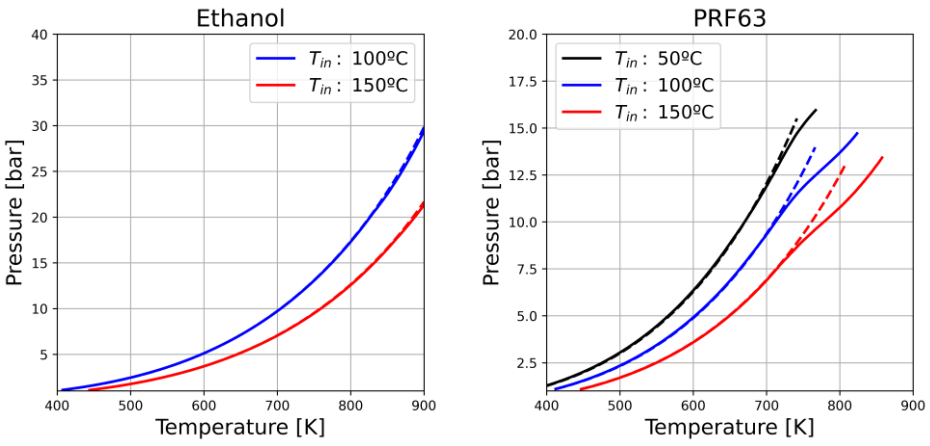

Figure 15. Comparison of pressure-temperature trajectories generated in GT-Power for motored conditions against the equivalent burning case for ethanol (a) and PRF63 (b).

In this sense, both (experimental and simulated) boundary conditions were used for the LW methodology aiming at quantifying the impact of the differences in the pressure temperature trajectory on the ignition delays determination. Figure 16 presents the results for both ethanol (Figure 16 a) and for PRF63 (Figure 16 b) considering the species that represents the early reactions of each fuel. As it can be seen, for ethanol, the use of the boundary conditions generated by the GT-Power model seems to have a proper agreement with those from the experiments. This may be attributed to the absence of LTHR of ethanol and its low energy release at intermediate temperature range. Nonetheless, an offset can be evidenced, leading to delayed ignition times which might be related to the fact that early reactions that leads to the hydrogen peroxide formation are not considered in the calculation.

A similar behavior can be observed for PRF63. First, the proposed methodology demonstrates the capability of reproducing with high accuracy the low temperature ignition delay, even if the non-reactive boundary conditions are used for the calculations. As in the Ethanol case, PFR 63 also demonstrates to be shifted to delayed conditions. This is mainly justified by the fact that the species used to quantify the low temperature ignition delay (Hydroperoxyl, HO_2) is not one of the first species to be formed during the hydrocarbon oxidation. Nonetheless, the pre-reactions associated to radicals like keto-hydroperoxide (HPMF, $HOOCH_2OCHO$) or carbonic acid (HOC(O)OH) [71][72], in general, provides a much lower reliability due to the difficulty of quantifying the proper reaction rates of this species due to their low concentration.

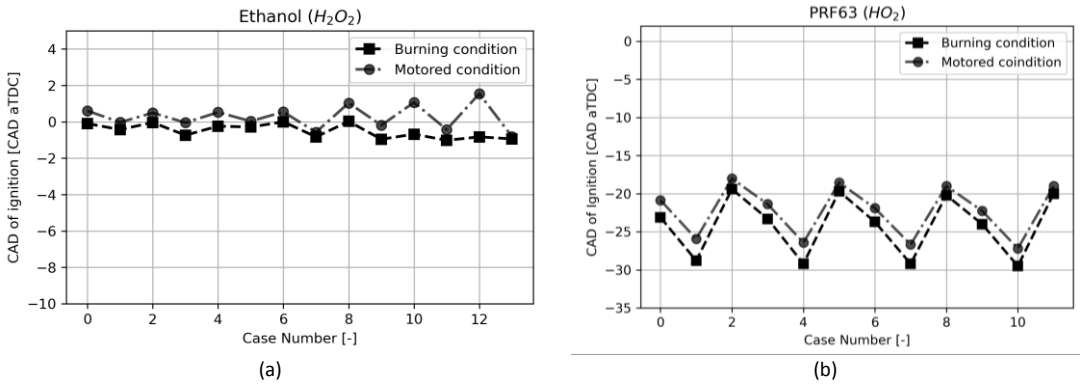

Figure 16. Start of combustion predicted pressure-temperature trajectories of burning cases and motored cases for ethanol (a) and PRF63 (b).

5. Conclusions

This work has proposed and validated a specific framework to evaluate the fuel response to different homogenous charge compression ignition conditions by means of a coupled 1-D CFD and reaction Kinetics solver for Livengood and Wu calculations. Fuels with single and two stage oxidations were tested aiming at calculating the low, intermediate, and high temperature ignition delay, if is the case. Moreover, different techniques to improve the calculation speed were implemented, quantifying the impact on the ignition delay determination. The different analysis has allowed to draw important remarks summarized as:

- The use of the proposed methodology enables the investigation of different fuels in terms of reaction Kinetics, allowing to characterize the different ignition delays.
- Low temperature ignition delay for two stage oxidation fuels has been determined with negligible differences with respect to the experimental database.
- The use of simple correlations has been proven as a successful approach for non-sensitive fuels. On the other hand, sensitive fuels with NTC have demonstrated a high deviation, requiring alternatives such as the use of tabulated chemistry to successfully determine the ignition delay.
- Look-up tables showed the best trade-off between computational time and generalization, enabling their application independently of the fuel.

Finally, the use of non-reactive boundary conditions from GT-Power simulations was assessed to quantify its capability on determining the early oxidation reactions for both fuels. It can be concluded that the proposed methodology has been proven a successful framework to identify potential fuels in terms of its response to the different operating conditions, considering its ignition delay time quantifications. The proposed methodology can assist the development and refinement of low temperature combustion concepts, allowing to understand the interplay between fuels and operating conditions found in engines. This certainly can also offer a pathway to refine and identify possible low carbon fuels with similar characteristics to run in advanced combustion concepts, resulting not only in low criteria pollutants but also reductions in green house gases emissions.

Acknowledgements

This work has been partially funded by Spanish Ministry of Science, Innovation and Universities under the "Salvador de Madariaga" grant (PRX18/00131) and by the Swedish Energy Agency under the project “Future Alternative Transportation Fuels” and the project number 41139-1. The project partners were F3, Lantmännen, Perstorp AB, Preem, Scania AB, st1, Saybolt Sweden AB, Stena Line, Volvo AB, and Volvo Cars.

References

[1] International Energy Agency (IEA), “Global EV Outlook 2020: Entering the decade of electric drive?,” *Glob. EV Outlook 2020*, p. 273, 2020.

[2] P. K. Senecal and F. Leach, “Diversity in transportation: Why a mix of propulsion technologies is the way forward for the future fleet,” *Results Eng.*, vol. 4, no. October, p. 100060, 2019, doi: 10.1016/j.rineng.2019.100060.

[3] ExxonMobil, “2019 Outlook for energy: a perspective to 2040,” 2019.

[4] The European Comission, “REGULATIONS. Commission regulations (EU) 2019/318 of February 2019 amending Regulation (EU) 2017/2400 and Directive 2007/46/EC of the European Parliament and of the Council as regards the determination of the CO2 emission and fuel cunsumption of heavy-dut,” *Off. J. Eur. Union*, vol. 2001, no. May, pp. 20–30, 2019, doi: http://eur-lex.europa.eu/pri/en/oj/dat/2003/l_285/l_28520031101en00330037.pdf.

[5] The European Comission, “COMBINED EVALUATION ROADMAP/ INCEPTION IMPACT ASSESSMENT,” 2020.

[6] V. B. Pedrozo, X. Wang, W. Guan, and H. Zhao, “The effects of natural gas composition on conventional dual-fuel and reactivity-controlled compression ignition combustion in a heavy-duty diesel engine,” *Int. J. Engine Res.*, 2021, doi: 10.1177/1468087420984044.

[7] R. García-Contreras, J. A. Soriano, P. Fernández-Yáñez, A. Gómez, O. Armas, and M. D. Cárdenas, “Impact of regulated pollutant emissions of Euro 6d-Temp light-duty diesel vehicles under real driving conditions,” *J. Clean. Prod.*, vol. 286, 2021, doi: 10.1016/j.jclepro.2020.124927.

[8] M. Li, Z. Wei, X. Liu, X. Wang, Q. Zhang, and Z. Li, “A numerical investigation on the effects of gaseous fuel composition in a pilot ignited direct injection natural gas engine,” *Energy*, vol. 217, no. July, p. 106961, 2021, doi: 10.1016/j.energy.2020.119467.

[9] J. Wan, Y. Zhuang, Y. Huang, Y. Qian, and L. Qian, “A review of water injection application on spark-ignition engines,” *Fuel Process. Technol.*, vol. 221, no. July, p. 106956, 2021, doi: 10.1016/j.fuproc.2021.106956.

[10] J. Benajes, A. García, J. Monsalve-Serrano, and S. Martínez-Boggio, “Emissions reduction from passenger cars with RCCI plug-in hybrid electric vehicle technology,” *Appl. Therm. Eng.*, vol. 164, no. August 2019, p. 114430, 2020, doi: 10.1016/j.applthermaleng.2019.114430.

[11] X. Li, B. Q. He, and H. Zhao, “Effect of direct injection dimethyl ether on the micro-flame ignited (MFI) hybrid combustion characteristics of an optical gasoline engine at ultra-lean conditions,” *Fuel Process. Technol.*, vol. 203, no. 92, p. 106383, 2020, doi: 10.1016/j.fuproc.2020.106383.

[12] S. H. Park, I. M. Youn, Y. Lim, and C. S. Lee, “Influence of the mixture of gasoline and diesel fuels on droplet atomization, combustion, and exhaust emission characteristics in a compression ignition engine,” *Fuel Process. Technol.*, vol. 106, pp. 392–401, 2013, doi: 10.1016/j.fuproc.2012.09.004.

[13] S. Simsek, S. Uslu, H. Simsek, and G. Uslu, “Improving the combustion process by determining the optimum percentage of liquefied petroleum gas (LPG) via response surface methodology (RSM) in a spark ignition (SI) engine running on gasoline-LPG blends,” *Fuel Process. Technol.*, vol. 221, no. June, p. 106947, 2021, doi: 10.1016/j.fuproc.2021.106947.

[14] J. J. López, J. M. García-Oliver, A. García, and V. Domenech, “Gasoline effects on spray characteristics, mixing and auto-ignition processes in a CI engine under Partially Premixed Combustion conditions,” *Appl. Therm. Eng.*, vol. 70, no. 1, pp. 996–1006, 2014, doi: 10.1016/j.applthermaleng.2014.06.027.

[15] F. C. P. Leach, M. H. Davy, and M. S. Peckham, “Cyclic NO2:NOx ratio from a diesel engine undergoing transient load steps,” *Int. J. Engine Res.*, vol. 22, no. 1, pp. 284–294, 2021, doi: 10.1177/1468087419833202.

[16] M. Krishnamoorthi, R. Malayalamurthi, Z. He, and S. Kandasamy, “A review on low temperature combustion engines: Performance, combustion and emission characteristics,” *Renew. Sustain. Energy Rev.*, vol. 116, no. October, p. 109404, 2019, doi: 10.1016/j.rser.2019.109404.

[17] A. Calle-Asensio, J. J. Hernández, J. Rodríguez-Fernández, M. Lapuerta, A. Ramos, and J. Barba, “Effect of advanced biofuels on WLTC emissions of a Euro 6 diesel vehicle with SCR under different climatic conditions,” *Int. J. Engine Res.*, 2021, doi: 10.1177/14680874211001256.

[18] P. Zhang, J. He, H. Chen, X. Zhao, and L. Geng, “Improved combustion and emission characteristics of ethylene glycol/diesel dual-fuel engine by port injection timing and direct injection timing,” *Fuel Process. Technol.*, vol. 199, no. November 2019, p. 106289, 2020, doi: 10.1016/j.fuproc.2019.106289.

[19] R. Chen, K. Nishida, and B. Shi, “Characteristics of combustion and soot formation of ethanol-gasoline blends injected by a hole-type nozzle for direct-injection spark-ignition engines,” *Fuel Process. Technol.*, vol. 181, no. August, pp. 318–330, 2018, doi: 10.1016/j.fuproc.2018.10.011.

[20] M. Yao, Z. Zheng, and H. Liu, “Progress and recent trends in homogeneous charge compression ignition (HCCI) engines,” *Prog. Energy Combust. Sci.*, vol. 35, no. 5, pp. 398–437, 2009, doi: 10.1016/j.pecs.2009.05.001.

[21] R. D. Reitz and G. Duraisamy, “Review of high efficiency and clean reactivity controlled compression ignition (RCCI) combustion in internal combustion engines,” *Prog. Energy Combust. Sci.*, vol. 46, pp. 12–71, 2015, doi: 10.1016/j.pecs.2014.05.003.

[22] A. García, J. Monsalve-Serrano, R. Lago Sari, and P. Gaillard, “Assessment of a complete truck operating under dual-mode dual-fuel combustion in real life applications: Performance and emissions analysis,” *Appl. Energy*, vol. 279, no. August, p. 115729, 2020, doi: 10.1016/j.apenergy.2020.115729.

[23] A. García, J. Monsalve-Serrano, D. Villalta, and R. Lago Sari, “Performance of a conventional diesel aftertreatment system used in a medium-duty multi-cylinder dual-mode dual-fuel engine,” *Energy Convers. Manag.*, vol. 184, 2019,

doi: 10.1016/j.enconman.2019.01.069.

[24] J. Benajes, A. García, J. Monsalve-Serrano, and R. Sari, “Clean and efficient dual-fuel combustion using OMEx as high reactivity fuel: Comparison to diesel-gasoline calibration,” *Energy Convers. Manag.*, vol. 216, no. May, p. 112953, 2020, doi: 10.1016/j.enconman.2020.112953.

[25] D. Lopez Pintor, J. Dec, and G. Gentz, “ϕ-sensitivity for LTGC engines: Understanding the fundamentals and tailoring fuel blends to maximize this property,” *SAE Tech. Pap.*, vol. 2019-April, no. April, pp. 1–24, 2019, doi: 10.4271/2019-01-0961.

[26] J. E. Dec, G. Gentz, and D. Lopez-pintor, “Low-Temperature Gasoline Combustion (LTGC) Engine Research,” 2018.

[27] A. Calam, “Study on the combustion characteristics of acetone/n-heptane blend and RON50 reference fuels in an HCCI engine at different compression ratios,” *Fuel*, vol. 271, no. January, p. 117646, 2020, doi: 10.1016/j.fuel.2020.117646.

[28] X. Duan, M. C. Lai, M. Jansons, G. Guo, and J. Liu, “A review of controlling strategies of the ignition timing and combustion phase in homogeneous charge compression ignition (HCCI) engine,” *Fuel*, vol. 285, no. September 2020, p. 119142, 2021, doi: 10.1016/j.fuel.2020.119142.

[29] P. W. Bessonette, C. H. Schleyer, K. P. Duffy, W. L. Hardy, and M. P. Liechty, “Effects of fuel property changes on heavy-duty HCCI combustion,” *SAE Tech. Pap.*, vol. 2007, no. 724, pp. 776–790, 2007, doi: 10.4271/2007-01-0191.

[30] D. Carney, “Mazda’s New Skyactiv-X Engine Gives New Life to Internal Combustion,” *IEEE Spectr.*, 2018, [Online]. Available: https://spectrum.ieee.org/transportation/efficiency/mazdas-new-skyactivx-engine- gives-new-life-to-internal-combustion.

[31] A. Solouk, M. Shakiba-Herfeh, J. Arora, and M. Shahbakhti, “Fuel consumption assessment of an electrified powertrain with a multi-mode high-efficiency engine in various levels of hybridization,” *Energy Convers. Manag.*, vol. 155, no. November 2017, pp. 100–115, 2018, doi: 10.1016/j.enconman.2017.10.073.

[32] M. Christensen, A. Hultqvist, and B. Johansson, “Demonstrating the multi fuel capability of a homogeneous charge compression ignition engine with variable compression ratio,” *SAE Tech. Pap.*, no. 724, 1999, doi: 10.4271/1999-01-3679.

[33] G. Mittal, M. Chaos, C. J. Sung, and F. L. Dryer, “Dimethyl ether autoignition in a rapid compression machine: Experiments and chemical kinetic modeling,” *Fuel Process. Technol.*, vol. 89, no. 12, pp. 1244–1254, 2008, doi: 10.1016/j.fuproc.2008.05.021.

[34] A. García, J. Monsalve-Serrano, E. José Sanchís, and Á. Fogué-Robles, “Exploration of suitable injector configuration for dual-mode dual-fuel engine with diesel and OMEx as high reactivity fuels,” *Fuel*, vol. 280, no. June, p. 118670, 2020, doi: 10.1016/j.fuel.2020.118670.

[35] A. García, A. Gil, J. Monsalve-Serrano, and R. Lago Sari, “OMEx-diesel blends as

high reactivity fuel for ultra-low NOx and soot emissions in the dual-mode dual-fuel combustion strategy," *Fuel*, vol. 275, no. February, p. 117898, 2020, doi: 10.1016/j.fuel.2020.117898.

[36] J. Liu *et al.*, "Effects of PODE/diesel blends on particulate matter emission and particle oxidation characteristics of a common-rail diesel engine," *Fuel Process. Technol.*, vol. 212, no. June 2020, p. 106634, 2021, doi: 10.1016/j.fuproc.2020.106634.

[37] M. Pochet, I. Truedsson, F. Foucher, F. Contino, and V. U. Brussel, "Ammonia-Hydrogen Blends in Homogeneous-Charge Compression-Ignition Engine," 2020, doi: 10.4271/2017-24-0087.Copyright.

[38] J. Pan, H. Wei, G. Shu, Z. Chen, and P. Zhao, "The role of low temperature chemistry in combustion mode development under elevated pressures," *Combust. Flame*, vol. 174, pp. 179–193, 2016, doi: 10.1016/j.combustflame.2016.09.012.

[39] C. Jin and Z. Zheng, "A Review on Homogeneous Charge Compression Ignition and Low Temperature Combustion by Optical Diagnostics," *J. Chem.*, vol. 2015, 2015, p. e910348, 2015, doi: 10.1155/2015/910348, 10.1155/2015/910348.

[40] J. O. Olsson *et al.*, "Compression ratio influence on maximum load of a natural gas fueled HCCI engine," *SAE Tech. Pap.*, vol. 2002, no. 724, 2002, doi: 10.4271/2002-01-0111.

[41] S. Cheng *et al.*, "Autoignition behavior of gasoline/ethanol blends at engine-relevant conditions," *Combust. Flame*, vol. 216, pp. 369–384, 2020, doi: 10.1016/j.combustflame.2020.02.032.

[42] G. Shibata, K. Oyama, T. Urushihara, and T. Nakano, "Correlation of low temperature heat release with fuel composition and HCCI engine combustion," *SAE Tech. Pap.*, vol. 2005, no. 724, 2005, doi: 10.4271/2005-01-0138.

[43] I. Truedsson, W. Cannella, B. Johansson, and M. Tuner, "Development of New Test Method for Evaluating HCCI Fuel Performance," *SAE Tech. Pap.*, vol. 2014-Octob, 2014, doi: 10.4271/2014-01-2667.

[44] S. Tanaka, F. Ayala, J. C. Keck, and J. B. Heywood, "Two-stage ignition in HCCI combustion and HCCI control by fuels and additives," *Combust. Flame*, vol. 132, no. 1–2, pp. 219–239, 2003, doi: 10.1016/S0010-2180(02)00457-1.

[45] M. Mikulski and C. Bekdemir, "Understanding the role of low reactivity fuel stratification in a dual fuel RCCI engine – A simulation study," *Appl. Energy*, vol. 191, pp. 689–708, 2017, doi: 10.1016/j.apenergy.2017.01.080.

[46] M. Mikulski, S. Ramesh, and C. Bekdemir, "Reactivity Controlled Compression Ignition for clean and efficient ship propulsion," *Energy*, vol. 182, pp. 1173–1192, 2019, doi: 10.1016/j.energy.2019.06.091.

[47] J. Krasselt, D. Foster, J. Ghandhi, R. Herold, D. Reuss, and P. Najt, "Investigations into the effects of thermal and compositional stratification on HCCI combustion - Part I: Metal engine results," *SAE Tech. Pap.*, vol. 2, no. 1, 2009, doi:

10.4271/2009-01-1105.

[48] M. Sjöberg and J. E. Dec, “Combined effects of fuel-type and engine speed on intake temperature requirements and completeness of bulk-gas reactions for HCCI combustion,” *SAE Tech. Pap.*, vol. 2003, no. 724, 2003, doi: 10.4271/2003-01-3173.

[49] J. L. S. Fagundez, R. L. Sari, A. Garcia, F. M. Pereira, M. E. S. Martins, and N. P. G. Salau, “A chemical kinetics based investigation on laminar burning velocity and knock occurrence in a spark-ignition engine fueled with ethanol–water blends,” *Fuel*, vol. 280, no. May, p. 118587, 2020, doi: 10.1016/j.fuel.2020.118587.

[50] G. Technologies, “Engine_Performance manual.” 2016.

[51] S. Salih and D. Delvescovo, “Design and Validation of a GT Power Model of the CFR Engine towards the Development of a Boosted Octane Number,” *SAE Tech. Pap.*, vol. 2018-April, pp. 1–21, 2018, doi: 10.4271/2018-01-0214.

[52] R. K. T. Morel, C.I.Rackmil and M. J. Jennings, “Model for Heat Transfer and Combustion in Spark Ignited Engines and Its Comparison with Experiments,” *SAE Tech. Pap. Ser.*, 1988.

[53] J. C. G. Andrae, “Comprehensive chemical kinetic modeling of toluene reference fuels oxidation,” *Fuel*, vol. 107, pp. 740–748, 2013, doi: 10.1016/j.fuel.2013.01.070.

[54] M. Tao, P. Zhao, D. DelVescovo, and H. Ge, “Manifestation of octane rating, fuel sensitivity, and composition effects for gasoline surrogates under advanced compression ignition conditions,” *Combust. Flame*, vol. 192, no. March, pp. 238–249, 2018, doi: 10.1016/j.combustflame.2018.02.015.

[55] J. C. Livengood and P. C. Wu, “Correlation of autoignition phenomena in internal combustion engines and rapid compression machines,” *Symp. Combust.*, vol. 5, no. 1, pp. 347–355, 1955, doi: 10.1016/S0082-0784(55)80047-1.

[56] R. M. Hanson and R. D. Reitz, “Effects of biofuel blends on transient reactivity-controlled compression ignition engine combustion,” *Int. J. Engine Res.*, vol. 17, no. 8, pp. 857–865, 2016, doi: 10.1177/1468087415622340.

[57] J. Benajes, A. García, J. Monsalve-Serrano, I. Balloul, and G. Pradel, “Evaluating the reactivity controlled compression ignition operating range limits in a high-compression ratio medium-duty diesel engine fueled with biodiesel and ethanol,” *Int. J. Engine Res.*, vol. 18, no. 1–2, pp. 66–80, 2017, doi: 10.1177/1468087416678500.

[58] J. B. Heywood, *Internal Combustion Engine Fundementals*, vol. 21. 1988.

[59] D. Vuilleumier *et al.*, “Intermediate temperature heat release in an HCCI engine fueled by ethanol/n-heptane mixtures: An experimental and modeling study,” *Combust. Flame*, vol. 161, no. 3, pp. 680–695, 2014, doi: 10.1016/j.combustflame.2013.10.008.

[60] N. Peters, G. Paczko, R. Seiser, and K. Seshadri, “Temperature cross-over and

non-thermal runaway at two-stage ignition of n-heptane," *Combust. Flame*, vol. 128, no. 1–2, pp. 38–59, 2002, doi: 10.1016/S0010-2180(01)00331-5.

[61] M. U. Waqas, A. Hoth, C. P. Kolodziej, T. Rockstroh, J. P. Gonzalez, and B. Johansson, "Detection of low Temperature heat release (LTHR) in the standard Cooperative Fuel Research (CFR) engine in both SI and HCCI combustion modes," *Fuel*, vol. 256, no. August, p. 115745, 2019, doi: 10.1016/j.fuel.2019.115745.

[62] J. M. Desantes, V. Bermúdez, J. J. López, and D. López-Pintor, "A new method to predict high and low-temperature ignition delays under transient thermodynamic conditions and its experimental validation using a Rapid Compression-Expansion Machine," *Energy Convers. Manag.*, vol. 123, pp. 512–522, 2016, doi: 10.1016/j.enconman.2016.06.051.

[63] M. Blocquet, C. Schoemaecker, D. Amedro, O. Herbinet, F. Battin-Leclerc, and C. Fittschen, "Quantification of OH and HO2 radicals during the low-temperature oxidation of hydrocarbons by Fluorescence assay by Gas Expansion technique," *Proc. Natl. Acad. Sci. U. S. A.*, vol. 110, no. 50, pp. 20014–20017, 2013, doi: 10.1073/pnas.1314968110.

[64] X. Yang, W. Liang, T. Tan, and C. K. Law, "Reevaluation of the reaction rate of H + O2 (+M) = HO2 (+M) at elevated pressures," *Combust. Flame*, vol. 217, pp. 103–112, 2020, doi: 10.1016/j.combustflame.2020.03.018.

[65] D. M. Manias, E. Al Tingas, C. E. Frouzakis, K. Boulouchos, and D. A. Goussis, "The mechanism by which CH2O and H2O2 additives affect the autoignition of CH4/air mixtures," *Combust. Flame*, vol. 164, pp. 111–125, 2016, doi: 10.1016/j.combustflame.2015.11.008.

[66] Z. J. Buras, C. Safta, J. Zádor, and L. Sheps, "Simulated production of OH, HO2, CH2O, and CO2 during dilute fuel oxidation can predict 1st-stage ignition delays," *Combust. Flame*, vol. 216, pp. 472–484, 2020, doi: 10.1016/j.combustflame.2019.12.013.

[67] M. Mikulski, P. R. Balakrishnan, and J. Hunicz, "Natural gas-diesel reactivity controlled compression ignition with negative valve overlap and in-cylinder fuel reforming," *Appl. Energy*, vol. 254, no. July, p. 113638, 2019, doi: 10.1016/j.apenergy.2019.113638.

[68] P. Jeanney, L. Magne, N. Moreau, S. Pasquiers, and P. Tardiveau, "Ignition of Lean Air / Hydrocarbon Mixtures at Low Temperature by a Single Corona Discharge Nanosecond Pulse," *AerospaceLab*, no. 10, pp. 1–8, 2015.

[69] F. S. Shariatmadar, S. G. Pakdehi, and M. A. Zarei, "An Empirical Correlation to Predict the Ignition Delay Time for Some Hydrocarbon Fuels," vol. 13, no. 1, pp. 84–97, 2016.

[70] D. DelVescovo, S. Kokjohn, and R. Reitz, "The Development of an Ignition Delay Correlation for PRF Fuel Blends from PRF0 (n-Heptane) to PRF100 (iso-Octane)," *SAE Int. J. Engines*, vol. 9, no. 1, pp. 520–535, 2016, doi: 10.4271/2016-01-0551.

[71] K. Moshammer *et al.*, “Detection and Identification of the Keto-Hydroperoxide (HOOCH2OCHO) and Other Intermediates during Low-Temperature Oxidation of Dimethyl Ether,” *J. Phys. Chem. A*, vol. 119, no. 28, pp. 7361–7374, 2015, doi: 10.1021/acs.jpca.5b00101.

[72] H. J. Curran, P. Gaffuri, W. J. Pitz, and C. K. Westbrook, “A comprehensive modeling study of n-heptane oxidation,” *Combust. Flame*, vol. 114, no. 1–2, pp. 149–177, 1998, doi: 10.1016/S0010-2180(97)00282-4.

Abbreviatures

aTDC: After Top Dead Centre

CAD: Crank Angle Degree

CA50: Crank Angle for 50% completion of combustion

CFR: Cooperative Fuel Research

CH_2O: formaldehyde

CO_2: carbon dioxide

CR: Compression Ratio

ECU: Electronic Control Unit

HCCI: Homogeneous Charge Compression Ignition

HOC(O)OH: Carbonic acid

$HOOCH_2OCHO$: Keto-hydroperoxide

HO_2: hydroperoxyl radical

H_2O_2: hydrogen peroxide

HTHR: High Temperature Heat Release

HTID: High Temperature Ignition Delay

ITHR: Intermediate Temperature Heat Release

ITID: Intermediate Temperature Ignition Delay

LTHR: Low Temperature Heat Release

LTID: Low Temperature Ignition Delay

LW: Livengood and Wu

NO: Nitrogen monoxide

NO_2: nitrogen dioxide

NO_x: nitrogen oxides

NTC: Negative Temperature Coefficient

MON: Motor Octane Number

OH: hydroxyl radical

PRF: Primary Reference Fuel

RCCI: Reactivity Controlled Compression Ignition

RON: Research Octane Number

TPA: Three Pressure Analysis

Symbols

P: Pressure

T: Temperature

Y: Mass Fraction

τ: Ignition Delay

ϕ: Relative Fuel-to-Air ratio

λ: Relative Air-to-Fuel ratio